

Bond between ribbed bars and concrete. Part 1: Modified model  
K. Lundgren

Published in Magazine of Concrete Research, see journal homepage  
<http://www.icevirtuallibrary.com/content/journals>

"Permission is granted by ICE Publishing to print one copy for personal use. Any other use of these PDF files is subject to reprint fees."

# Bond between ribbed bars and concrete. Part 1: Modified model

K. Lundgren\*

Chalmers University of Technology, Göteborg, Sweden

The bond between ribbed bars and concrete is influenced by a number of parameters, such as the strength of the surrounding structure, the occurrence of splitting cracks, and yielding of the reinforcement. A model for three-dimensional analyses was developed earlier by the author, where the splitting stresses of the bond action were included, and the bond stress depended not only on the slip but also on the radial deformation between the reinforcement bar and the concrete. The bond model, however, was shown to generate energy for some special loading–unloading sequences. This undesirable effect has led to a change in the formulation of the bond model. With the modification as described here, the model becomes equivalent to the Coulomb friction, complemented with a yield function describing the upper limit. Pull-out tests were analysed, using the modified bond model and non-linear fracture mechanics for the concrete. The tests were selected to show various types of failure: pull-out failure, splitting failure, pull-out failure after yielding of the reinforcement, rupture of the reinforcement bar, and cyclic loading. The results show that the modified model is capable of predicting splitting failures, and the loss of bond if the reinforcement is yielding, as well as simulating cyclic loading in a physically reasonable way.

## Notation

		$u_n$	relative normal displacement at the interface
$c$	parameter in yield function $F_2$ (the stress in the inclined compressive struts)	$u_{nbond}$	normal deformation in the bond layer
		$u_t$	slip
		$u_{tbond}$	slip in the bond layer
$D_{11}, D_{22}, D_{33}$	stiffnesses in the elastic stiffness matrix	$u_{tmax}$	maximum value of the slip which has been obtained
$E_c$	modulus of elasticity of concrete	$u_{tmin}$	minimum value of the slip which has been obtained
$F_1$	yield line describing the friction		
$F_2$	yield line describing the upper limit at a pull-out failure	$\eta$	parameter in the plastic potential function $G$
$f_{cc}$	compressive strength of concrete	$\eta_{d0}$	the lowest value of the parameter $\eta$ in the damaged deformation zone
$G$	plastic potential function		
$\mathbf{t}$	the tractions at the interface	$\kappa$	hardening parameter
$t_n$	normal splitting stress	$\lambda$	plastic multiplier
$t_r$	stress in direction around the bar	$\mu$	coefficient of friction
$t_t$	bond stress	$\mu_{d0}$	the lowest value of the coefficient of friction in the damaged deformation zone
$\mathbf{u}$	the relative displacements across the interface		

\* Department of Civil and Environmental Engineering, Division of Structural Engineering, Concrete Structures, Chalmers University of Technology, SE-412 96 Göteborg, Sweden.

(MCR 31130) Paper received 29 April 2003; last revised 27 January 2004; accepted 24 February 2004

## Introduction

The bond mechanism is the interaction between reinforcement and the surrounding concrete. It is this transfer of stresses that makes it possible to combine the compressive strength of the concrete and the tensile

strength of the reinforcement in reinforced concrete structures. Thus, the bond mechanism has a strong influence on the fundamental behaviour of a structure, for example in crack development and spacing, crack width, and ductility. Bond action generates inclined forces which radiate outwards in the concrete. The inclined stress is often divided into a longitudinal component, denoted the bond stress, and a radial component, denoted normal stress or splitting stress. The inclined forces are balanced by tensile ring stresses in the surrounding concrete, as explained by Tepfers;<sup>1</sup> see Fig. 1. If the tensile stress becomes larger than the tensile strength of the concrete, longitudinal splitting cracks will form in the concrete.

It should be noted that the presence of the normal stresses is a condition for transferring bond stresses after the chemical adhesion is lost. When, for some reason, the normal stresses are lost, bond stresses cannot be transferred. This occurs if the concrete around the reinforcement bar is penetrated by longitudinal splitting cracks, and if there is no transverse reinforcement that can continue to carry the forces. This type of failure is called splitting failure. The same thing occurs if the reinforcement bar starts yielding. Due to the Poisson effect, the contraction of the steel bar increases drastically at yielding. Thus, the normal stress between the concrete and the steel is reduced so that only low bond stress can be transferred.

When the concrete surrounding the reinforcement bar is well-confined, meaning that it can withstand the normal splitting stresses, and the reinforcement does not start yielding, a pull-out failure is obtained. Under these conditions, the failure is characterised by shear cracking between the adjacent ribs. This is the upper limit of the bond strength.

A common way to describe the bond behaviour is by relating the bond stress to the slip, that is, the relative difference in movement between the reinforcement bar and the concrete. However, as made clear above, the bond versus slip relationship is not a material parameter; it is closely related to the structure. It also depends on several parameters such as casting position, vibration of the concrete and loading rate. Examples of schematic bond–slip relationships are shown in Fig. 2.

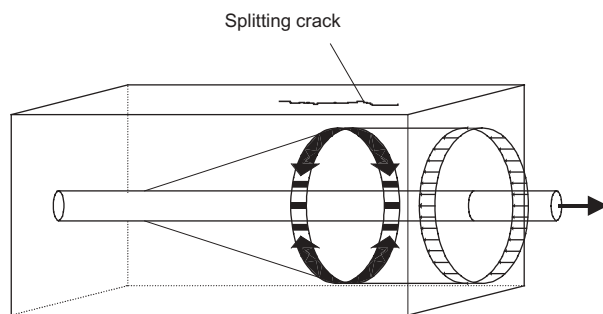


Fig. 1. Tensile ring stresses in the anchorage zone, according to Tepfers<sup>1</sup>

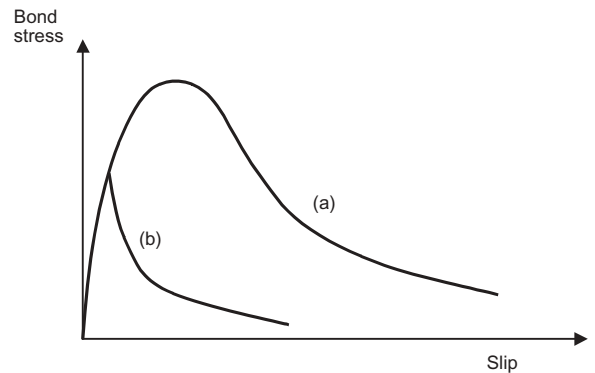


Fig. 2. Schematic bond–slip relationship: (a) pull-out failure; (b) splitting failure, or loss of bond due to yielding of the reinforcement

A model of the bond mechanism was developed by the author in earlier work; see Lundgren and Gylltoft.<sup>2</sup> The model includes the generated splitting stresses, and with the same input parameters, it results in various bond–slip curves, depending on the confinement of the surrounding structure, and on whether the reinforcement is yielding or not. The model has also been further developed to cover the behaviour of strands; see Gustavson.<sup>3</sup> The bond model, however, was shown to generate energy for some special loading–unloading sequences (Gustafsson P. J., pers. comm., 2002). To avoid this undesirable effect, the formulation of the bond model was modified. The modified formulation is presented here, together with results from analyses with the modified bond model for ribbed bars.

### Modified bond model

The modelling method used is specially suited for detailed three-dimensional finite element analyses, where both the concrete and the reinforcement are modelled with solid elements. Special interface elements were used at the surface between the reinforcement bars and the concrete to describe a relation between the traction  $\mathbf{t}$  and the relative displacement  $\mathbf{u}$  in the interface. The physical interpretations of the variables  $t_n$ ,  $t_t$ ,  $u_n$  and  $u_t$  are shown in Fig. 3. The interface elements have, initially, a thickness of zero.

#### Elasto-plastic formulation

The model of the bond mechanism is a frictional model, using elasto-plastic theory to describe the relations between the stresses and the deformations. It is a slight modification of the model presented by Lundgren and Gylltoft.<sup>2</sup> The reason for the modification was that with the original formulation of the model,<sup>2</sup> the model could, in special circumstances, generate energy (Gustafsson, pers. comm., 2002). This generation of energy occurs due to the asymmetric stiffness matrix, for special loading–unloading sequences within the elastic

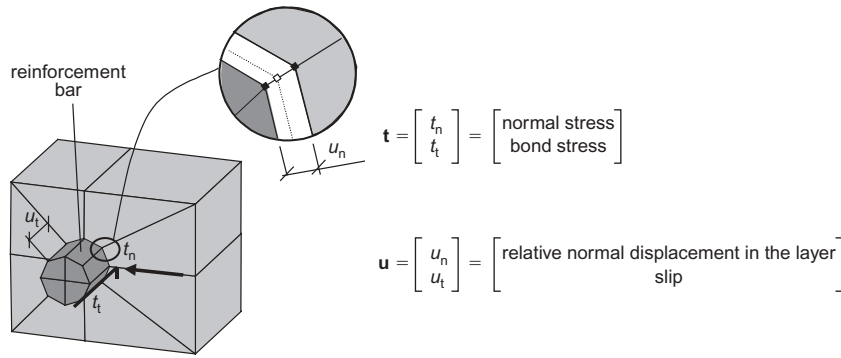


Fig. 3. Physical interpretation of the variables  $t_n$ ,  $t_t$ ,  $u_n$  and  $u_t$

region. One example of a loading sequence which generates energy when an asymmetric elastic matrix is used is the following

- Start with  $u_n = u_t = 0$ .
- $u_n = -1, u_t = 0$ .
- $u_n = -1, u_t = 1$ .
- $u_n = 0, u_t = 1$ .
- $u_n = 0, u_t = 0$ .

If the results obtained from these steps are within the elastic range, energy is generated in the  $u_n-t_n$  space, but not in the  $u_t-t_t$  space if the asymmetric stiffness matrix described by Lundgren and Gylltoft<sup>2</sup> is used. This is due to the fact that a slip ( $u_t$ ) gives a contribution to the normal stress ( $t_n$ ), whereas a normal deformation ( $u_n$ ) does not give any contribution to the bond stress ( $t_t$ ). Thus, in total, energy is created, which of course is an undesirable effect.

Therefore, the stiffness matrix was here changed into a symmetric one, so that the relation between the tractions  $\mathbf{t}$  and the relative displacements  $\mathbf{u}$  in the elastic range is

$$\begin{bmatrix} t_n \\ t_t \end{bmatrix} = \begin{bmatrix} D_{11} & 0 \\ 0 & D_{22} \end{bmatrix} \begin{bmatrix} u_{nbond} \\ u_{tbond} \end{bmatrix} \quad (1)$$

This is the only modification of the original model.<sup>2</sup>

Furthermore, the model has yield lines, flow rules and hardening laws. The yield lines are described by two yield functions, one describing the friction,  $F_1$ , assuming that the adhesion is negligible

$$F_1 = |t_t| + \mu t_n = 0 \quad (2)$$

The other yield line,  $F_2$ , describes the upper limit at a pull-out failure. This is determined from the stress in the inclined compressive struts that result from the bond action.

$$F_2 = t_t^2 + t_n^2 + c \cdot t_n = 0 \quad (3)$$

For plastic loading along the yield line describing the upper limit,  $F_2$ , an associated flow rule is assumed. For the yield line describing the friction,  $F_1$ , a non-

associated flow rule is assumed, where the plastic part of the deformations is

$$d\mathbf{u}^p = d\lambda \frac{\partial G}{\partial \mathbf{t}}, \quad G = \frac{|u_t|}{u_t} t_t + \eta t_n = 0 \quad (4)$$

where  $d\lambda$  is the incremental plastic multiplier. The yield lines are shown in Fig. 4. At the corners, a combination of the two flow rules is used; this is known as the Koiter rule.

For the hardening rule of the model, a hardening parameter  $\kappa$  is established. It is defined by

$$d\kappa = \sqrt{du_n^2 + du_t^2} \quad (5)$$

It can be noted that for monotonic loading,  $du_n^p$  and the elastic part of the slip are very small compared to the plastic part of the slip,  $du_t^p$ ; therefore the hardening parameter  $\kappa$  will be almost equivalent to the slip,  $u_t$ . The variables  $\mu$  and  $c$  in the yield functions are assumed to be functions of  $\kappa$ .

Three-dimensional modelling

For three-dimensional modelling, a third component is added: the stress acting in the direction around the bar. This, is assumed to act independently of the other components; thus, the equation for the elastic stage is then assumed to be

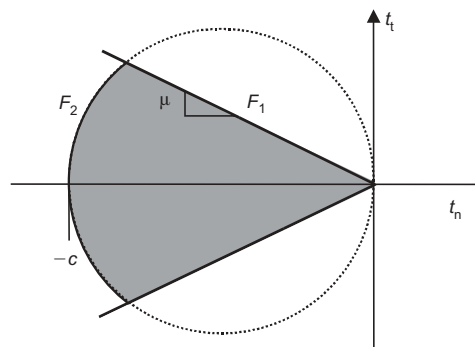


Fig. 4. The yield lines

$$\begin{bmatrix} t_n \\ t_t \\ t_r \end{bmatrix} = \begin{bmatrix} D_{11} & 0 & 0 \\ 0 & D_{22} & 0 \\ 0 & 0 & D_{33} \end{bmatrix} \begin{bmatrix} u_n \\ u_t \\ u_r \end{bmatrix} \quad (6)$$

The main objective with the stiffness  $D_{33}$  is that it prevents the bar from rotating in the concrete. The traction  $t_r$  has no influence on the yield lines.

*Damaged/undamaged deformation zones*

A typical bond–slip response for varying slip direction is with a steep unloading and then an almost constant, low bond stress until the original monotonic curve is reached; see Fig. 5(a). To make the model describe this typical response, the concept of damaged/undamaged deformation zones is used. The idea is that when the reinforcement slips in the concrete, the friction will be damaged in the range of the passed slip. This is a simplified way to describe the damage of the cracked and crushed concrete. In Fig. 5(b), the reinforcement is back in its original position after slipping in both directions. The concrete will then be crushed in the range of the passed slip. This crushed concrete still has some capacity to carry compressive load, but no capacity at all in tension. The friction is therefore assumed to vary in the damaged zone depending on whether loading is applied in the direction away from, or towards, the original position, as shown in Fig. 5(c)

and (d). The friction is assumed to drop immediately to a low value,  $\mu_{d0}$ , at load reversal, and to keep this value until the original position is reached. For further loading, away from the original position, the friction is assumed to increase gradually, until the undamaged zone is reached and the normal value of  $\mu$  is used again. To describe this gradual increase, an equation of the second degree was chosen.

The parameter  $\eta$  also has a lower value in the damaged deformation zone, varying in the same way as just described about the coefficient of friction. This lower value physically corresponds to the fact that the increase in the stresses is lower than in the undamaged deformation zone.

*Discussion of the modified bond model*

Note that with the modification of the model as described here (i.e. changing to a symmetric stiffness matrix), the model becomes equivalent to the Coulomb friction, complemented with the yield function describing the upper limit,  $F_2$ . Still, the model behaves very similarly to the original one. The most important feature of the model is that it applies to both the bond stress and the splitting stress, thus describing the inclined struts that result from the bond action. By modelling the surrounding structure, it is possible to obtain, for example, splitting cracks in the concrete, or cone

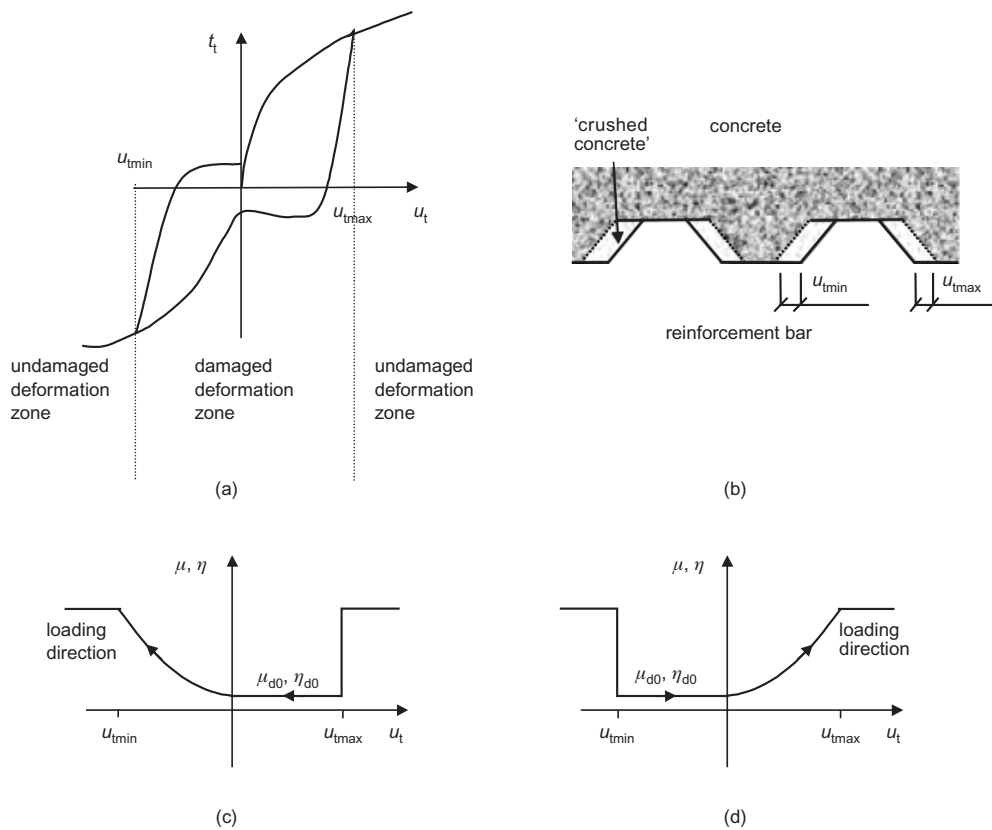


Fig. 5. (a) One load cycle with varying slip directions. (b) The reinforcement bar is back in its original position, after slipping in both directions. Maximum and minimum values of the slip are especially marked. (c, d) The parameters  $\mu$  and  $\eta$  vary within the damaged deformation zone depending on whether the loading is directed towards or away from the original position

cracks close to free edges. One of the main ideas of the model is that the complex crushing and cracking of the concrete close to the reinforcement bar are described in a simplified way by decreasing the friction between the reinforcement bar and the concrete. The model is sensitive to the resistance of the surrounding structure, so that if the pressure around the bar is lost for some reason, the bond stress will decrease.

One important difference, between the original proposed model and this modified model, is the normal stresses remaining after unloading of a pull-out force. They are much smaller when the original model is used. When the modified model is used, the normal stresses resulting from a pull-out force remain approximately the same if the pull-out force is unloaded.

*Input parameters for the interface*

The model is calibrated for reinforcement bars K500  $\phi$  16 and normal-strength concrete. However, the original model has also been used (without recalibration) for reinforcement bars of other dimensions, and for applications with high-strength concrete.<sup>4</sup> As the input used for the modified model for monotonic loading is the same as that described by Lundgren and Gylltoft<sup>2</sup> with the changes described by Lundgren,<sup>5</sup> this calibration will most likely apply also for other bar diameters and concrete strengths. Before using the values recommended here on, for example, fibre-reinforced concrete or other reinforcement qualities, analyses and comparisons with experimental results are recommended. In particular, changes would be needed if smooth instead of ribbed bars were considered.

For monotonic loading, there are five parameters in the model: the stiffnesses  $D_{11}$  and  $D_{22}$  in the elastic stiffness matrix  $\mathbf{D}$  in equation (1), the parameter  $\eta$  defined in equation (4), and the functions  $\mu(\kappa)$  and  $c(\kappa)$ . Of these,  $D_{22}$ ,  $\mu(\kappa)$  and  $c(\kappa)$  can be measured; see below on how they were determined.  $D_{11}$  and the parameter  $\eta$  have to be calibrated by analyses of experiments; however, for ribbed bars, they can be chosen within a rather large range without having any great influence on the behaviour. For cyclic loading, the parameters  $\eta_{d0}$  and  $\mu_{d0}$  are also needed.

First of all, the stiffness  $D_{22}$  in the elastic stiffness matrix  $\mathbf{D}$  was recognised as the stiffness of the first part, or at unloading, in a bond–slip curve. By assuming that this is proportional to the modulus of elasticity of the concrete, and by comparing with results from experiments, this stiffness was chosen to be

$$D_{22} = K_{22} \cdot E_c \tag{7}$$

where the parameter  $K_{22}$  was  $6.0 \text{ m}^{-1}$ . The stiffness  $D_{11}$  was assumed to be a function of the deformation  $u_n$ . This can physically be compared with the fact that normal pressure is obtainable only when there is contact between the two materials. If that rule was strictly followed, and penetration was not allowed, the stiffness  $D_{11}$  would be zero for positive values of the normal

deformation, and infinite when the normal deformation was zero. Such a definition of the stiffness would most likely lead to numerical problems. To reduce the problems, a maximum value of  $D_{11}$  was chosen for  $u_n$  smaller than zero, and  $D_{11}$  was decreased for positive  $u_n$  down to a minimum value, as shown in Fig. 6(a).

The variable  $c$  represents the stress in the inclined compressive struts. Thus, the maximum value of  $c(\kappa)$  is the compressive strength of the concrete; see Fig. 6(b). The functions  $\mu(\kappa)$  and  $c(\kappa)$  together result in the bond–slip curve at pull-out failure for ribbed bars.

The function  $\mu(\kappa)$  describes how the relation between the bond stress and the normal splitting stress depends on the hardening parameter. This can be measured indirectly in steel-encased pull-out tests. The chosen input is shown in Fig. 7. The parameter  $\eta$  describes the ability of the reinforcement to create normal stresses. It is chosen in order to obtain a decreasing bond stress when the concrete around the bar splits, without elastic unloading. Through calibration,  $\eta$  was chosen to be 0.04.

For cyclic loading,  $\eta_{d0}$  was chosen to be 0.002, and the coefficient of friction  $\mu_{d0}$  was 0.2. These parameters were the only ones that were changed relative to the earlier calibration; they were both halved. The reason for these changes is that, as the normal stresses are not unloaded when the slip is unloaded in the

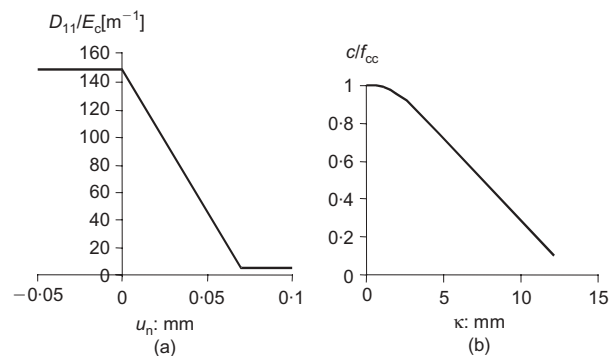


Fig. 6. (a) The stiffness  $D_{11}$ , and (b) the function  $c(\kappa)$

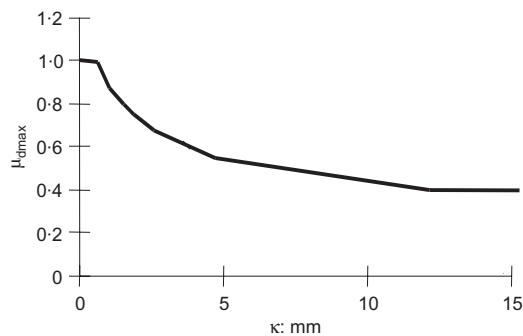


Fig. 7. Chosen input for the coefficient of friction as a function of the hardening parameter

modified model, the bond stresses obtained in the damaged zone were too large by comparison with experimental results when the old values were used.

For three-dimensional modelling, the stiffness  $D_{33}$  in equation (6) is also required. A value of  $10^{10} \text{ N m}^{-3}$  was used in all analyses, since it was found that this was enough to prevent the bar from rotating in the concrete.

## Comparison with tests

### *Finite element analyses*

Pull-out tests of various kinds were analysed with finite element models. The tests were selected to show various types of failure: pull-out failure, splitting failure, pull-out failure after yielding of the reinforcement, rupture of the reinforcement bar, and cyclic loading. In all tests, the reinforcement was of type K500  $\phi$  16, and the concrete was of normal strength (the compressive cylinder strength varies from 25 to 35 MPa).

From the various measured compressive strengths, an equivalent compressive cylinder strength,  $f_{cc}$ , was evaluated. Other necessary material data for the concrete were estimated according to the expressions in CEB<sup>6</sup> from  $f_{cc}$ . In all analyses, the concrete was modelled with a constitutive model based on non-linear fracture mechanics, using a rotating crack model based on total strain; see TNO.<sup>7</sup>

Most of the finite element models were axisymmetric; the only exception is the eccentric pull-out tests of Magnusson<sup>8</sup> (see section 'Splitting failure'). The main advantage when using axisymmetric models is that the calculation time required for the analyses is dramatically decreased. One disadvantage of axisymmetric models is that a certain number of discrete radial cracks must be assumed. In the analyses presented here, four radial cracks were assumed.

The constitutive behaviour of the reinforcement steel was modelled by the Von Mises yield criterion with associated flow and isotropic hardening. The elastic modulus of the reinforcement was assumed to be 200 GPa when it had not been measured.

### *Pull-out failure*

In tests carried out by the author,<sup>9</sup> reinforcement bars were pulled out of concrete cylinders surrounded by steel tubes. The steel tubes had a diameter of 70 mm, a height of 100 mm, and a thickness of 1.0 mm. The embedment length of the reinforcement bars was 50 mm. The tangential strains in the steel tubes were measured at three heights, together with the applied load and slip. Five tests were carried out, three in one direction and two in the other. When these tests were analysed, friction between the edges of the concrete and the support plates was considered, assuming the coefficient of friction to be 0.4. The friction at the supports did not influence the achieved load versus

slip; however, the tangential strains in the analyses were slightly influenced (increasing the friction at the supports led to larger strain in the middle of the zone with bond, and lower strains close to the supports). Results from the analyses, together with the finite element mesh used, are shown in Fig. 8. As can be seen, the agreement is rather good.

Pull-out tests carried out by Magnusson<sup>8</sup> and Balázs and Koch<sup>10</sup> were analysed. Magnusson had concrete cylinders with a diameter of 300 mm and an embedment length of 40 mm; Balázs and Koch had concrete specimens with a quadratic cross-section  $160 \times 160$  mm and an embedment length of 80 mm. In both cases, the concrete specimens were large enough to prevent splitting failure; thus, pull-out failures were obtained. Results from the analyses are compared with experiments in Fig. 9. As can be seen, reasonably good agreement was obtained.

### *Splitting failure*

Magnusson<sup>8</sup> has also carried out pull-out tests on eccentrically reinforced specimens with varying stirrup configurations. The different stirrup configurations (without stirrups, with two and with four stirrups along the embedment length) led to splitting failures at various levels. In the test specimen with four stirrups, the stirrups gave enough confinement to obtain a ductile failure after splitting. In the analyses of these experiments, the stirrups were modelled as embedded reinforcement, meaning that complete interaction between the stirrups and the concrete was assumed. The finite element model, together with the boundary conditions, is shown in Fig. 10(a). Since a smeared crack model was used, the input of a characteristic length was needed. This length should be related to the size of one element. This is based on an assumption that a crack will localise in one element. In these analyses, however, the crack localised in two elements. The characteristic length was therefore estimated to be 40 mm, based on the size of the area where the cracks localised; see Fig. 10(b). The results from these analyses are compared with test results in Fig. 11. It can be noted that even with the same embedment length, and when exactly the same input parameters were given for the interface, different load–slip curves were obtained depending on the modelled structure, in this case the number of stirrups. Comparing with the measured response, the agreement is good, especially when considering the large scatter that is always obtained in pull-out tests.

### *Yielding of the reinforcement*

Magnusson<sup>8</sup> has also conducted pull-out tests where the reinforcement had an embedment length long enough to give yielding of the reinforcement. Two of these tests were analysed, where the reinforcement was centrally placed in a concrete specimen of dimensions  $400 \text{ mm} \times 400 \text{ mm}$ . In one of the experiments, with an

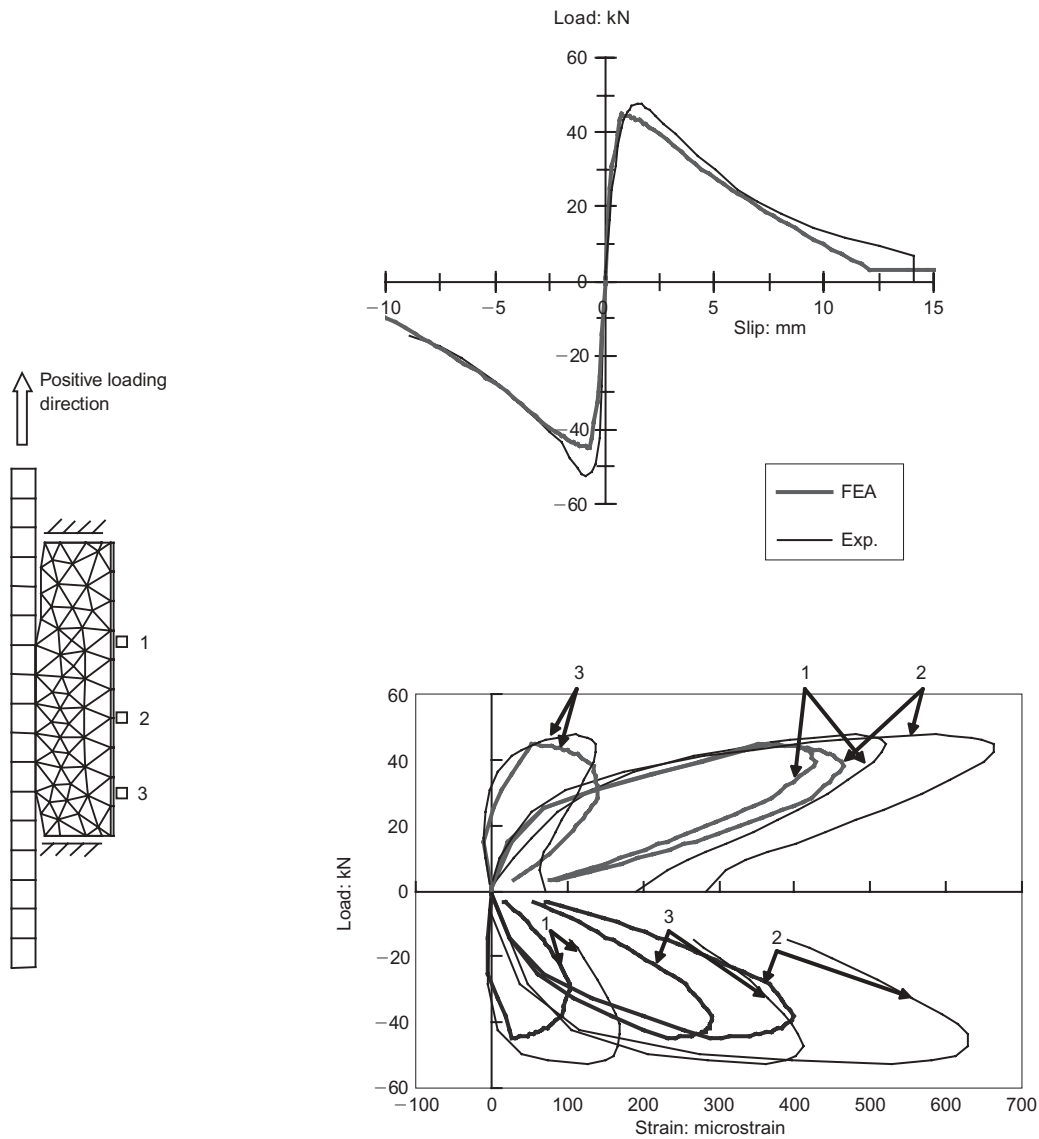


Fig. 8. Comparison between test results and results from the analyses of the monotonically loaded steel-encased pull-out tests

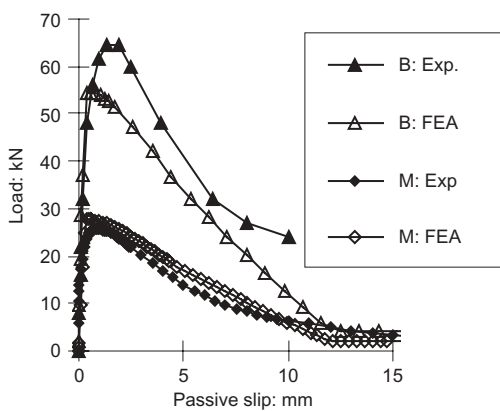


Fig. 9. Load versus slip in pull-out tests with short embedment length. B: Balázs and Koch<sup>10</sup> and M: Magnusson<sup>8</sup>

Magazine of Concrete Research, 2005, 57, No. 7

embedment length of 220 mm, a pull-out failure after yielding of the reinforcement was obtained; and in the other one, with an embedment length of 360 mm, rupture of the reinforcement bar occurred. As can be seen in Fig. 12, the same results were obtained in the analyses. In Fig. 13, the bond-slip resulting from the analyses at various levels along the bar is shown. It can be seen that the bond stress decreased drastically when the reinforcement reached the yield plateau. This is because the normal stress decreased when the radius of the reinforcement bar decreased. When the reinforcement began to harden again, a small bond capacity was obtained. This was possible since the decrease of the radius of the reinforcement was lower when the reinforcement hardened, and thus, normal stresses could be built up again.

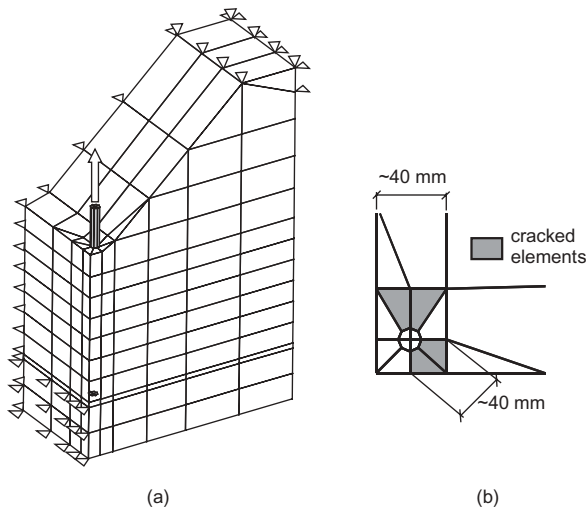


Fig. 10. (a) The finite element model of the pull-out tests on eccentrically reinforced specimens of Magnusson.<sup>8</sup> (b) Localisation of the main radial cracks in a cross-section

*Cyclic pull-out tests*

The steel-encased pull-out tests conducted by the author,<sup>9</sup> briefly described in the section ‘Pull-out failure’, were also carried out with reversed cyclic loading. The results from analyses of these experiments, using the rotating crack model for the concrete, are shown in Fig. 14. When the elasto-plastic Rankine material model was used for the concrete instead, the tangential strains in the steel tube were affected, especially after a few load cycles. Instead of a residual value of about 0.0%, about 0.5% was obtained. This can be compared to what was measured in the tests: about 0.25%. It was noted that especially the strain in the steel-encased tubes was changed when the modified bond model was used, compared with when the older version of the model was used. The reason for this change is that the normal stresses which result when a pull-out force is applied will not be unloaded if the pull-out force is unloaded when the modified model is used; see Fig.

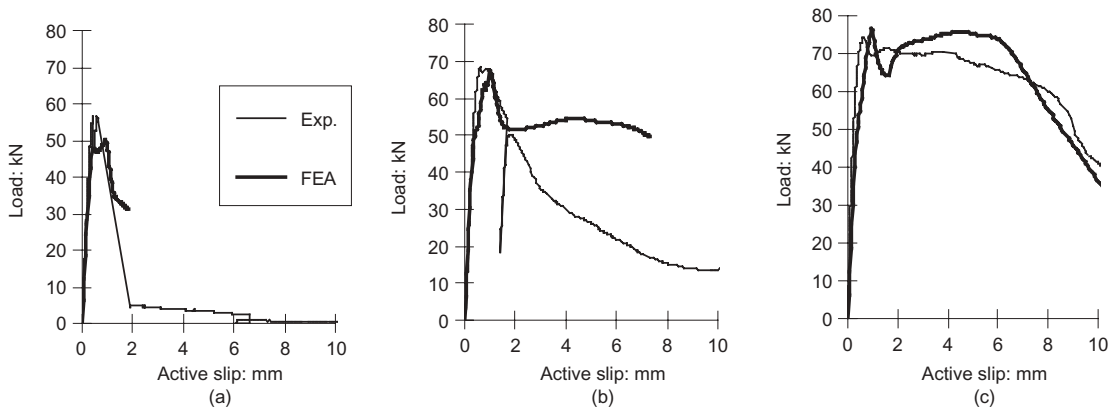


Fig. 11. Load versus slip in eccentrically reinforced pull-out tests. (a) Without stirrups; (b) with two stirrups; (c) with four stirrups

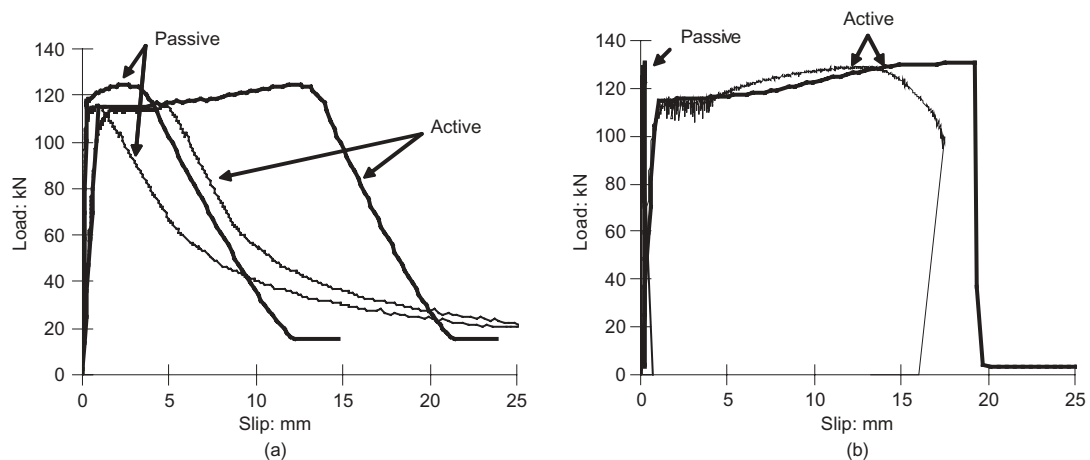


Fig. 12. Load versus slip in pull-out tests with long embedment length, thick lines for analyses and thin lines for test results. Experimental results from Magnusson.<sup>8</sup> (a) Embedment length 220 mm; (b) embedment length 360 mm

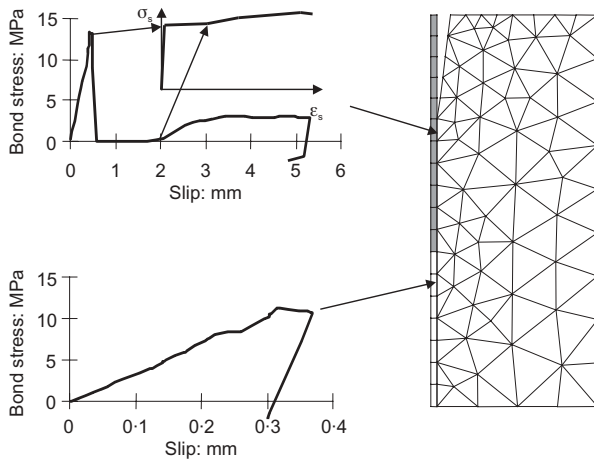


Fig. 13. Bond stress versus slip at various integration points along the bar in pull-out tests with embedment length 360 mm. The reinforcement elements that are marked grey reached yielding

15. However, the measured strain in the steel tubes depends both on how large the normal stresses are that remain at unloading, and on the behaviour of the concrete for cyclic loading. Therefore, it is difficult to judge from the measurements how large the normal stresses are that remain at unloading. To improve this, a concrete material model better suited for cyclic loading ought to be used. There is, however, no such model that is possible to use in these analyses implemented in the finite element programme today.

### Other influencing parameters

In the previous section, modelling results were compared to experimental results for tests that were selected to show five different types of failure: pull-out failure, splitting failure, pull-out failure after yielding of the reinforcement, rupture of the reinforcement bar, and cyclic loading. The results show that the model is capable of dealing with all these kinds of failure modes in a physically meaningful way, and reasonably good agreement between analyses and experimental results was found. On the other hand, there are further parameters that are known to influence the bond action. Two such parameters are the presence of outer pressure, and shrinkage of the concrete; although the model was not specifically calibrated with any tests for these two parameters, the behaviour of the model was observed in relation to their presence or absence.

#### Outer pressure

Pull-out tests with short embedment length (see Magnusson<sup>8</sup>) were analysed without any outer pressure, in the previous section. Here, an outer pressure of 5 MPa was applied and kept constant while the pull-out force was applied. The results are compared to results from the analysis without outer pressure; see Fig. 16. While the outer pressure was applied, the radial deformation between the reinforcement bar and the concrete decreased, which implies a normal stress  $t_n$ ; see Fig. 17. This means that, when slipping between the concrete and the reinforcement began, some normal stresses were already present. Therefore, the first part of the loading was elastic, until the yield line was reached. Thus, the load versus slip starts with a stiff, elastic part. The capacity, however, is not influenced, since the failure mode is pull-out failure in both cases; the pull-out failure in the model is governed by the upper limit in the form of the yield line,  $F_2$ , which is determined from the compressive strength of the concrete. Test results of Robins and Standish<sup>11</sup> indicate that this is a correct behaviour. They carried out cube pull-out tests with deformed bars with lateral pressure varying from 0 to 28 MPa. They concluded that the maximum capacity was increased for low levels of confinement, since the failure mode was changed from splitting failure to pull-out failure. On the other hand, further increase of the

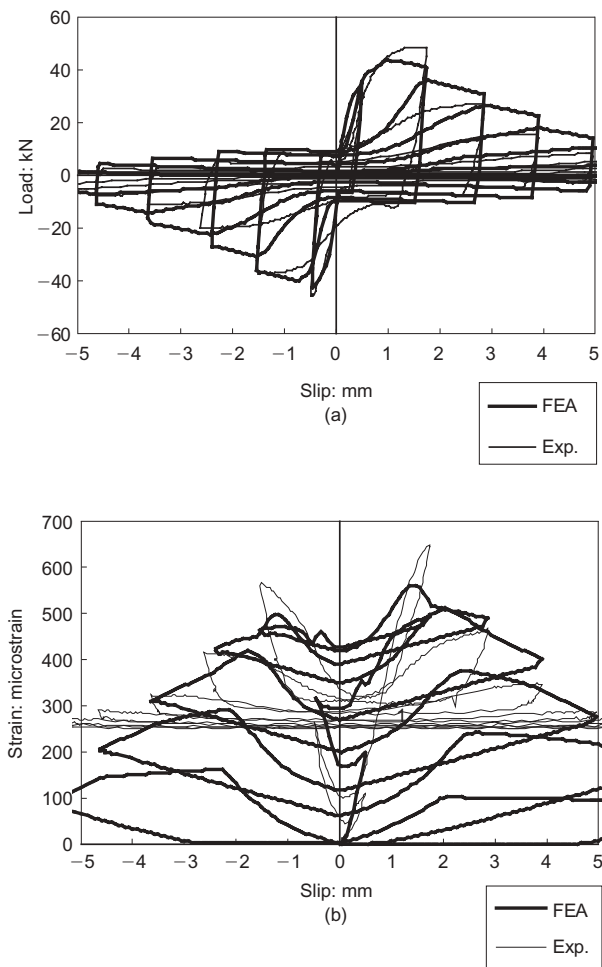


Fig. 14. Comparison between test results and results from the analysis of one cyclically loaded steel-encased pull-out test. (a) Load versus slip. (b) Tangential strain in the steel tube in the middle of the zone with bond

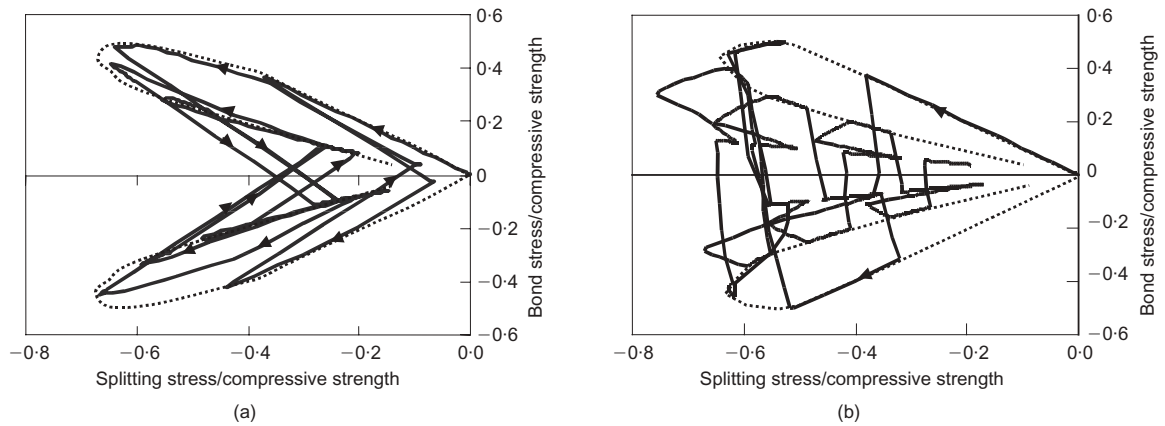


Fig. 15. The bond stress versus the splitting stress from the analyses of steel-encased pull-out tests (a) using the original model, and (b) using the modified model; solid lines for cyclic and dashed lines for monotonic loading

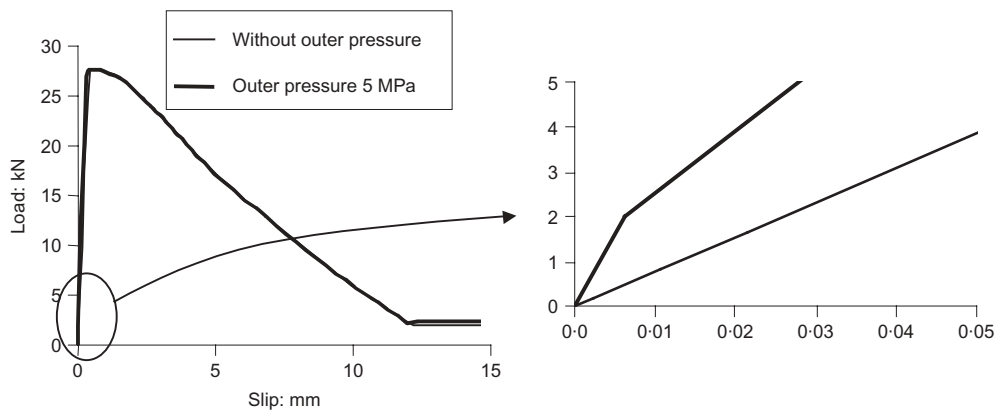


Fig. 16. Comparison of results from analyses of a pull-out test where pull-out failure is limiting, with and without an outer pressure

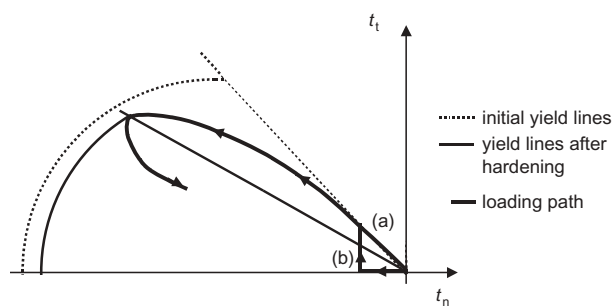


Fig. 17. The effect of either outer pressure or shrinkage of the concrete, in the stress space: (a) without outer pressure or shrinkage of the concrete, and (b) with either an outer pressure or shrinkage of the concrete taken into account

lateral confinement had no influence on the maximum capacity.

There are tests described in the literature that report a higher capacity due to outer pressure. However, when these references were read more thoroughly, it appeared

that splitting cracks were present; see Untrauer and Henry,<sup>12</sup> Eligehausen *et al.*<sup>13</sup> As these splitting cracks had probably reduced the capacity, the presence of an outer pressure would have a beneficial effect. This also reflects the behaviour of the model presented. A pull-out test similar to Magnusson's one with short embedment length,<sup>8</sup> but with a reduced cover, was analysed both with and without a confining outer pressure. The cover in these analyses was 30 mm. In the analysis without outer pressure, failure was due to splitting of the concrete. As can be seen in Fig. 18, an outer pressure then increased the capacity. In this example, the applied outer pressure was great enough to prevent the development of splitting cracks; thus, the capacity was increased to the level of a pull-out failure. For a low confining pressure, the formation of the splitting cracks would only have been delayed, meaning that the capacity would have been greater than for the unconfined specimen although not enough to lead to a pull-out failure.

The results here are similar to those obtained with

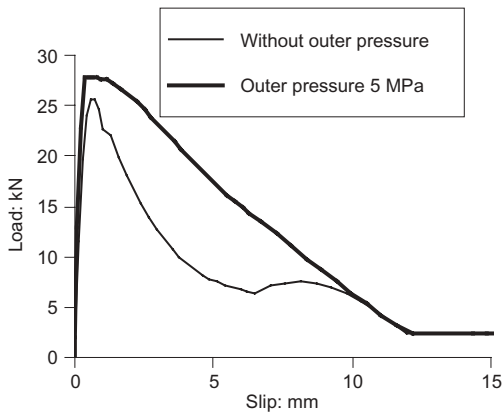


Fig. 18. Comparison of results from analyses of a pull-out test where splitting failure is limiting, with and without an outer pressure

the original bond model. In Lundgren and Magnusson,<sup>4</sup> the original model was applied in analyses of beam ends. The beam ends were either supported at their lower edge, so that the support reaction gave confinement to the reinforcement anchored over the support, or they were hung so that the support reaction acted over the reinforcement bars; that is, there was no confinement. It appeared from the analyses that the model could describe the behaviour accurately, and reasonably good agreement was found between the analyses and the test results. When no confinement was present, splitting failure occurred, which reduced the anchorage capacity in both the analyses and the tests. The confinement made it possible to obtain a pull-out failure in the analyses; that is, the capacity was increased by about as much as in the tests. From these tests and analyses, it seems that the model can also describe the effect of outer pressure in a reasonable way. The results

indicate that outer pressure can increase the bond capacity to the limit of the pull-out failure, although no further.

*Shrinkage*

The adhesion between the concrete and the reinforcement bar is assumed to be negligible for ribbed bars. On the other hand, in pull-out tests it is usual to have a first part of the load versus slip curve that is very stiff; this part is usually said to be due to the adhesion. However, a part of it may be caused by shrinkage of the concrete. When the concrete around the reinforcement bar shrinks, there are normal stresses between the concrete and the reinforcement bar before slipping starts. This resembles the situation with outer pressure discussed before; see Fig. 17. Yet there is a difference, namely that the shrinkage of the concrete also causes tensile stresses around the reinforcement bar, so that splitting cracks may appear. This is in contrast to the application of outer pressure which does not give rise to any tensile stresses.

The pull-out test with short embedment length (see Magnusson<sup>8</sup>) was analysed both with and without shrinkage of the concrete being taken into account. A shrinkage strain of  $-1.1 \times 10^{-5}$  was then applied, calculated according to CEB,<sup>6</sup> taking into account how the test specimens were stored. The results are compared in Fig. 19. As can be seen, the first part is stiffer when shrinkage is taken into account. However, for larger values of the slip, there is no difference between the two analyses.

**Conclusions**

A bond model for three-dimensional analyses, developed earlier by the author, was shown to generate

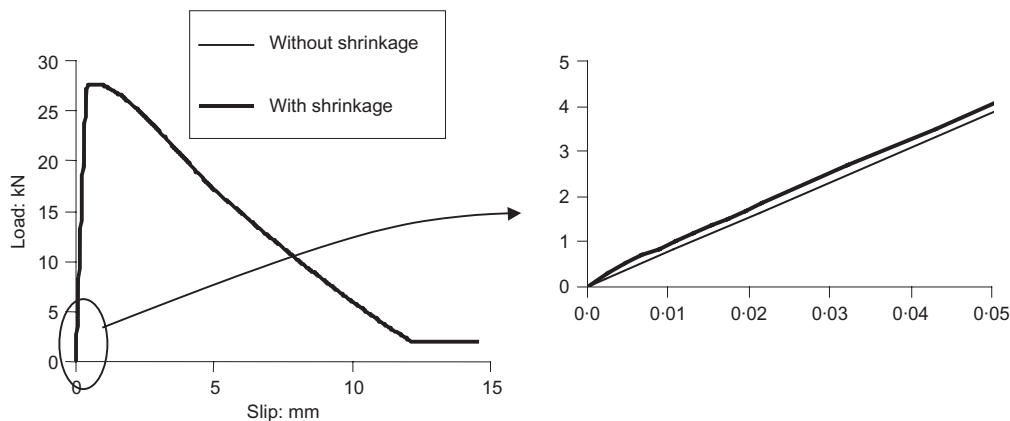


Fig. 19. The results from analysis of a pull-out test, with and without shrinkage of the concrete taken into account

energy for some special loading–unloading sequences. To avoid this, the bond model was modified. With the modification as described here, the model becomes equivalent to the Coulomb friction, complemented with the yield function describing the upper limit. The analyses carried out by Lundgren and Gylltoft,<sup>2</sup> namely pull-out tests selected to show various types of failure, were re-analysed with this modification of the model. For all the monotonically loaded specimens, no effect on the results was found. However, for the cyclically loaded specimens, some effects were noted. Cyclically loaded steel-encased pull-out tests, where the tangential strain in the steel tubes had been measured, were used. It was noted that especially the strain in the steel-encased tubes was changed when the modified bond model was used, in comparison with the results obtained when the older version of the model was used. However, it was concluded that a concrete material model better suited for cyclic loading ought to be used to improve the calibration for cyclic loading.

In conclusion, the agreement is rather good when comparing results from analyses with the measured response from different experiments. The failure mode is the same as in experiments in all of the analyses carried out. The results show that the modified model is capable of predicting splitting failures, and the loss of bond if the reinforcement is yielding, as well as simulating cyclic loading in a physically reasonable way.

### Acknowledgement

The author wishes to thank Professor Per Johan Gustafsson, Lund Institute of Technology, for his comments about the original bond model.

### References

1. TEPFERS R. *A Theory of Bond Applied to Overlapped Tensile Reinforcement Splices for Deformed Bars*. PhD thesis, Division of Concrete Structures, Chalmers University of Technology, Göteborg, 1973.
2. LUNDGREN K. and GYLLTOFT K. A model for the bond between concrete and reinforcement. *Magazine of Concrete Research*, 2000, **52**, No. 1, 53–63.
3. GUSTAVSON R. *Structural Behaviour of Concrete Railway Sleepers*. PhD thesis, Department of Structural Engineering, Chalmers University of Technology, Göteborg, 2002.
4. LUNDGREN K. and MAGNUSSON J. Three-dimensional modelling of anchorage zones in reinforced concrete. *ASCE Journal of Engineering Mechanics*, 2001, **127**, No. 7, 693–699.
5. LUNDGREN K. Modelling the effect of corrosion on bond in reinforced concrete. *Magazine of Concrete Research*, 2002, **54**, No. 3, 165–173.
6. CEB. *CEB-FIP Model Code 1990*. Bulletin d'Information 213/214, Lausanne, Switzerland, 1993.
7. TNO. *DIANA Finite Element Analysis, User's Manual release 7*. TNO Building and Construction Research, The Hague, 1998.
8. MAGNUSSON J. *Bond and Anchorage of Ribbed Bars in High-Strength Concrete*. PhD thesis, Division of Concrete Structures, Chalmers University of Technology, Göteborg, 2000.
9. LUNDGREN K. Pull-out tests of steel-encased specimens subjected to reversed cyclic loading. *Materials and Structures*, 2000, **33**, No. 231, 450–456.
10. BALÁZS G. and KOCH R. Bond characteristics under reversed cyclic loading. *Otto Graf Journal*, 1995, **6**, No. 1, 47–62.
11. ROBINS P. J. and STANDISH I. G. The influence of lateral pressure upon anchorage bond. *Magazine of Concrete Research*, 1984, **36**, No. 129, 195–202.
12. UNTRAUER R. E. and HENRY R. L. Influence of normal pressure on bond strength. *Journal of the ACI*, 1965, **62**, No. 5, 577–586.
13. ELIGEHAUSEN R., POPOV E. P. and BERTERO V. V. *Local Bond Stress-Slip Relationships of Deformed Bars under Generalized Excitations*. Earthquake Engineering Research Centre, University of California, Berkeley, California, USA UCB/EERC 83/23, October 1983.

**Discussion contributions on this paper should reach the editor by 1 March 2006**